Discovery of novel A3 adenosine receptor ligands based on chromone scaffold

ARTICLE *in* BIOCHEMICAL PHARMACOLOGY · MARCH 2012

Impact Factor: 5.01 · DOI: 10.1016/j.bcp.2012.03.007 · Source: PubMed

Biochemical Pharmacology 84 (2012) 21–29

Contents lists available at SciVerse ScienceDirect

Biochemical Pharmacology

journal homepage: www.elsevier.com/locate/biochempharm

Discovery of novel A_3 adenosine receptor ligands based on chromone scaffold

Alexandra Gaspar [a], Joana Reis [a], Sonja Kachler [c], Silvia Paoletta [d], Eugenio Uriarte [a,b,c,d], Karl-Norbert Klotz [c], Stefano Moro [d], Fernanda Borges [a,*]

[a] CIQUP/Departamento de Química e Bioquímica, Faculdade de Ciências, Universidade do Porto, 4169-007 Porto, Portugal
[b] Departamento de Química Orgánica, Facultad de Farmacia, Universidad de Santiago de Compostela, 15782 Santiago de Compostela, Spain
[c] Institut für Pharmakologie und Toxikologie, Universität Würzburg, 97078 Würzburg, Germany
[d] Molecular Modeling Section (MMS), Dipartimento di Scienze Farmaceutiche, Università di Padova, via Marzolo 5, I-35131 Padova, Italy

ARTICLE INFO

Article history:
Received 27 January 2012
Accepted 9 March 2012
Available online 17 March 2012

Keywords:
Drug discovery
Adenosine receptor ligand
Chromone scaffold

ABSTRACT

A project focused on the discovery of new chemical entities (NCEs) as AR ligands that incorporate a benzo-γ-pyrone [(4H)-1-benzopyran-4-one] substructure has been developed. Accordingly, two series of novel chromone carboxamides placed at positions C2 (compounds **2**–**13**) and C3 (compounds **15**–**26**) of the γ-pyrone ring were synthesized using chromone carboxylic acids (compounds **1** or **14**) as starting materials. From this study and on the basis of the obtained structure–activity relationships it was concluded that the chromone carboxamide scaffold represent a novel class of AR ligands. The most remarkable chromones were compounds **21** and **26** that present a better affinity for A_3AR (K_i = 3680 nM and K_i = 3750 nM, respectively). Receptor-driven molecular modeling studies provide information on the binding/selectivity data of the chromone. The data so far acquired are instrumental for future optimization of chromone carboxamide as a selective A_3AR antagonist.

1. Introduction

Cancer is a very complex disease, linked with different initiating causes, cofactors and promoters, and several types of cellular damage. Advancing knowledge on the cellular and molecular biology of the processes that regulate cell proliferation, cell differentiation and cellular responses to external signals provide a wealth of information about the biochemistry and biology of the cancer cell and how it differs from a normal one [1]. Accordingly, a number of potential targets as well as the development of a new generation of anticancer agents must be exploited, based on the differences between normal and cancer cells [2].

During the last decade different approaches to treating cancer have been developed based mainly on specific targets that are mostly expressed in tumor but not in normal cells [2]. Interestingly, it was already shown that adenosine receptor (AR) levels in various tumor cells are up regulated, a finding which may suggest that a specific AR may serve as a biological marker and as a target for specific ligands leading to cell growth inhibition [3]. In particular, the human A_3 AR, which is the most recently identified adenosine receptor, is involved in a variety of important physiological processes that include inflammation, cell growth and immunosuppression [4–7].

There have been many attempts to design and develop A_3 AR agonists and antagonists, and over the past decade, the search for ligands that show selectivity toward individual receptor subtypes has intensified as their role in many therapeutic areas expands [4,8,9]. Despite the intense discovery efforts the overall process has failed to deliver selective (agonists or antagonists) drug candidates, with exception of CF102 (1-[2-chloro-6-[[(3-iodophenyl)methyl]amino]-9*H*-purin-9-yl]-1-deoxy-*N*-methyl-β-D-ribofuran uronamide, Cl-IB-MECA) that is in clinical trials [4,10,11]. Main problems include side effects due to the ubiquity of the receptors or to low absorption, short half-life and toxicity of the ligands [10]. These facts prompted an intensive research effort

Abbreviations: [^{3}H]CCPA, [^{3}H](2R,3R,4S,5R)-2-[2-chloro-6-(cyclopentylamino)-purin-9-yl]-5-(hydroxymethyl)oxolane-3,4-diol; [^{3}H]HEMADO, [^{3}H] 2-(1-Hexynyl)-*N*^{6}-methyladenosine; [^{3}H]NECA, [^{3}H]adenosine-5′-(*N*-ethylcarboxamide); AR, Adenosine receptor; Arg, arginine; Asn, asparagine; Asp, aspartic acid; BBr_3, boron tribromide; BOP, (benzotriazol-1-yloxy)tris(dimethylamino)phosphonium hexafluorophosphate; CHO, Chinese hamster ovary cells; Cys, cysteine; DAD, diode-array detector; DIPEA, *N*,*N*-diisopropylethylamine; DMF, dimethylformamide; EI-MS, electron impact mass spectra; Glu, glutamic acid; HPLC, high performance liquid chromatography; Ile, isoleucine; K_i, inhibition constant; Leu, leucine; MOE, molecular operating environment; MOPAC, molecular orbital PACkage; NCE, new chemical entity; NMR, nuclear magnetic resonance; PLANTS, protein-Ligand ANT System; Phe, phenylalanine; Pro, proline; PyBOP, benzotriazol-1-yloxytripyrrolidinophosphonium hexafluorophosphate; R-PIA, *N*-R-*N*^{6}-(1-methyl-2-phenylethyl)adenosine; SAR, structure–affinity relationship; TLC, thin layer chromatography; TMS, tetramethylsilane; Trp, tryptophan; Tyr, tyrosine; UV, ultraviolet; ZM241385, 4-(2-[7-Amino-2-(2-furyl)[1,2,4]triazolo[2,3-a][1,3,5]triazin-5-ylamino]ethyl)phenol.

* Corresponding author at: CIQ/Department of Chemistry and Biochemistry, Faculty of Sciences, University of Porto, Porto 4169-007, Portugal.
Tel.: +351 220402560.
E-mail address: fborges@fc.up.pt (F. Borges).

0006-2952/$ – see front matter © 2012 Elsevier Inc. All rights reserved.
doi:10.1016/j.bcp.2012.03.007

toward the development of novel, selective and potent AR receptor ligands suitable for chemotherapeutic purposes.

Concurrently, despite the steady increase in R&D expenditures within the pharmaceutical industry, the number of new chemical entities (NCEs) reaching the market has actually decreased dramatically. Therefore, privileged structures, such as indoles, arylpiperazines, biphenyls and benzopyranes (*e.g.* coumarins and chromones), are currently considered as potentially successful approaches in drug discovery and have been used successfully before in medicinal chemistry programs to identify NCEs [12].

Accordingly, a project focused on the discovery of NCEs as AR ligands that incorporate a benzo-γ-pyrone [(4*H*)-1-benzopyran-4-one] substructure has been developed. Based on knowledge acquired so far no information on the development of putative adenosine ligands based on this type of scaffold have been reported, concerning the flavonoid family. However, flavonoids are natural secondary metabolites that possess a C6–C3–C6 skeleton. The present chromone series possess some structural similarities with flavones, namely the presence of A and C rings, but the B ring is absent.

Therefore, the aim of the present study is the design and synthesis of a library of novel adenosine receptor ligands based on the chromone scaffold that was obtained through the application of innovative synthetic strategies (Scheme 1) [13]. Lead discovery of new AR ligands based on a chromone scaffold guided by structure–affinity-relationships (SAR) and molecular modeling is the aim of the present work.

2. Materials and methods

2.1. Materials

Chromone-2-carboxylic and chromone-3-carboxylic acids, (benzotriazol-1-yloxy)tris(dimethylamino)phosphonium hexafluorophosphate (BOP), benzotriazol-1-yloxytripyrrolidinophosphonium hexafluorophosphate (PyBOP), *N*,*N*-diisopropylethylamine (DIPEA), dimethylformamide (DMF), boron tribromide (BBr_3), aniline and its derivatives were purchased from Sigma–Aldrich Química S.A. (Sintra, Portugal). All other reagents and solvents were *pro analysis* grade and were acquired from Merck (Lisbon, Portugal) and used without additional purification.

Thin-layer chromatography (TLC) was carried out on pre-coated silica gel 60 F254 (Merck, Lisbon, Portugal) with layer thickness of 0.2 mm. For analytical control the following systems were used: ethyl acetate/petroleum ether, ethyl acetate/methanol, chloroform/methanol in several proportions. The spots were visualized under UV detection (254 and 366 nm) and iodine vapor. Normal-phase column chromatography was performed using silica gel 60 0.2–0.5 or 0.040–0.063 mm (Merck, Lisbon, Portugal).

The purity of the final products (>97% purity) was verified by high-performance liquid chromatography (HPLC) equipped with a UV detector. Chromatograms were obtained in an HPLC/DAD system, a Jasco instrument (pumps model 880-PU and solvent mixing model 880-30, Tokyo, Japan), equipped with a commercially prepacked Nucleosil RP-18 analytical column (250 mm × 4.6 mm, 5 μm, Macherey-Nagel, Duren, Germany), and UV detection (Jasco

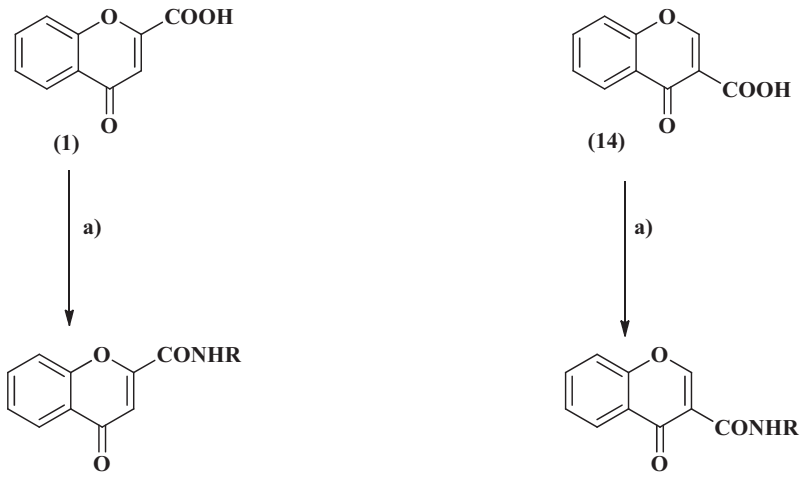

(2) R=Ph
(3) R=C_6H_{11}
(4) R=C_3H_7
(5) R=(4'-OH-Ph)
(6) R=(4'-OCH_3-Ph)
(7) R=(4'-CH_3-Ph)
(8) R=(3'-OH-4'-OCH_3-Ph)
(9) R=(3',4'-OCH_3-Ph)
(10) R=(4'-Cl-Ph)
(11) R=(4'-OCF_3-Ph)
(12) R=(4'-CF_3-Ph)
(13) R=(4'-NO_2-Ph)

(15) R=Ph
(16) R=C_6H_{11}
(17) R=C_3H_7
(18) R=(4'-OH-Ph)
(19) R=(4'-OCH_3-Ph)
(20) R=(4'-CH_3-Ph)
(21) R=(3'-OH-4'-OCH_3-Ph)
(22) R=(3',4'-OCH_3-Ph)
(23) R=(4'-Cl-Ph)
(24) R=(4'-OCF_3-Ph)
(25) R=(4'-CF_3-Ph)
(26) R=(4'-NO_2-Ph)

(a) R-NH_2, BOP or PyBOP, DIPEA in DCM/DMF

Scheme 1. Structure of the chromone carboxamides under study.

model 875-UV) at the maximum wavelength of 254 nm. The mobile phase consisted of a methanol/water or acetonitrile/water (gradient mode, room temperature) at a flow rate of 1 mL/min. The chromatographic data was processed in a Compaq computer, fitted with CSW 1.7 software (DataApex, Czech Republic). ^{1}H NMR data were acquired, at room temperature, on a Brüker AMX 300 spectrometer operating at 300.13 MHz, respectively. Dimethylsulfoxide-d_6 was used as a solvent; chemical shifts are expressed in δ (ppm) values relative to tetramethylsilane (TMS) as internal reference; coupling constants (J) are given in Hz. Electron impact mass spectra (EI-MS) were carried out on a VG AutoSpec instrument; the data are reported as m/z (% of relative intensity of the most important fragments). Melting points were obtained on a Stuart Scientific SMP1 apparatus and are uncorrected.

2.2. Synthesis of chromone carboxamide derivatives

General procedure: 2-Carboxychromone (**1**) or 3-carboxychromone (**14**) (0.50 g; 2.63 mmol) was dissolved in of DMF (6 mL) and of DIPEA (0.37 mL). The solution was then cooled at 0 °C in an ice-water bath, and a BOP (1.16 g; 2.63 mmol) or PyBOP (1.37 g; 2.63 mmol) solution in CH_2Cl_2 (6 mL) was added. The mixture was stirred during 30 min. After, the phenylamine derivative was added in equimolar amount. The temperature was gradually increased to room temperature. The reaction was stirred for additional 4 h. Following the workup and after extraction, the organic phases were dried over Na_2SO_4. Solutions were decolorized with activated charcoal, when necessary. The recrystallization solvents were ethyl acetate or ethyl ether/n-hexane.

2.2.1. N-(4-Methoxyphenyl)-4-oxo-4H-1-benzopyran-2-carboxamide (6)

Yield: 85%; MP: 214–223 °C; ^{1}H NMR ($CDCl_3$): 3.83 (3H, *s*, OCH_3), 6.94 (2H, *d*, *J* = 9.2, H(3′), H(5′)), 7.27 (1H, *s*, H(3)), 7.49 (1H, *ddd*, *J* = 8.0; 7.2; 1.0, H(6)), 7.59–7.64 (3H, *m*, H(8), H(2′), H(6′)), 7.78 (1H, *ddd*, *J* = 8.5; 7.1; 1.6, H(7)), 8.25 (1H, *dd*, *J* = 8.0, 1.6, H(5)), 8.53 (1H, *s*, NH). MS/EI *m*/*z* (int.rel.): 296 (14), 295 ($M^{\bullet+}$, 100), 294 (30), 266 (15), 173 (13), 145 (10), 122 (68), 95 (17), 89 (22), 71 (10), 69 (11), 57 (15).

2.2.2. N-(4-Methylphenyl)-4-oxo-4H-1-benzopyran-2-carboxamide (7)

Yield: 56%; MP: 233–237 °C; ^{1}H NMR [$(CD_3)_2SO$]: 2.30 (3H, *s*, CH_3), 6.97 (1H, *s*, H(3)), 7.23 (2H, *d*, *J* = 8.2, H(3′), H(5′)), 7.57 (1H, *ddd*, *J* = 7.9, 7.0, 1.0, H(6)), 7.69 (2H, *d*, *J* = 8.3, H(2′), H(6′)), 7.85 (1H, *dd*, *J* = 8.5, 1.0, H(8)), 7.93 (1H, *ddd*, *J* = 8.5, 7.0, 1.5, H(7)), 8.08 (1H, *dd*, *J* = 8.0, 1.4, H(5)), 10.68 (1H, *s*, NH); MS/EI *m*/*z* (int.rel.): 280 (32), 279 ($M^{\bullet+}$, 100), 278 (94), 264 (10), 262 (29), 251 (11), 250 (46), 233 (14), 158 (17), 107 (10), 106 (35), 89 (53), 79 (14), 77 (20).

2.2.3. N-(3,4-Dimethoxyphenyl)-4-oxo-4H-1-benzopyran-2-carboxamide (9)

Yield: 45%; MP: 196–198 °C; ^{1}H NMR [$(CD_3)_2SO$]: 3.77/3.79 (6H, 2 *s*, 2× OCH_3), 6.97 (1H, *s*, H (3)), 7.01 (1H, *d*, *J* = 8.7, H(5′)), 7,40 (1H, *dd*, *J* = 8.7; 2.4, H(6′)), 7.48 (1H, *d*, *J* = 2.4, H(2′)), 7.58 (1H, *ddd*, *J* = 8.0, 6.8, 1.2, H(6)), 7,.86 (1H, *d*, *J* = 7.7, H(8)), 7.95 (1H, *ddd*, *J* = 8.5, 7.0, 1.6, H(7)), 8.10 (1H, *dd*, *J* = 8.0, 1.5, H(5)), 10.66 (1H, *s*, NH); MS/EI *m*/*z* (int.rel.): 326 (20), 325 ($M^{\bullet+}$, 100), 310 (21), 308 (15), 173 (24), 145 (22), 89 (37).

2.2.4. N-(4-Methoxyphenyl)-4-oxo-4H-1-benzopyran-3-carboxamide (19)

Yield: 55%; MP: 173–177 °C; ^{1}H NMR ($CDCl_3$): 3.84 (3H, *s*, OCH_3), 6.98 (2H, *d*, *J* = 9.0, H(3′), H(5′)), 7.25–7.32 (4H, *m*, H(6), H(8), H(2′), H(6′)), 7.59 (1H, *ddd*, *J* = 8.6, 6.9, 1.7, H(7)), 8.06/8.14 (1H, *dd*, *J* = 7.8, 1.6, H(5)), 8.80/8.94 (1H, *s*, H(2)), 11.95/13.76 (1H, *s*, NH), 13.76 (0.7H, *s*, NH); MS/EI *m*/*z* (int.rel.): 296 (55), 295 ($M^{\bullet+}$, 100), 280 (27), 252 (21), 174 (22), 173 (94), 147 (18), 132 (14), 121 (37), 92 (14), 77 (12).

2.2.5. N-(4-Methylphenyl)-4-oxo-4H-1-benzopyran-3-carboxamide (20)

Yield: 44%; MP: 179–182 °C; ^{1}H NMR ($CDCl_3$): 2.39 (3H, *s*, CH_3), 7.23–7.32 (6H, *m*, H(6), H(8), H(2′), H(3′), H(5′), H(6′), 7.60 (1H, *ddd*, *J* = 8.6, 7.0, 1.6, H(7)), 8.07/8.14 (1H, *dd*, *J* = 7.8, 1.6, H(5)), 8.86/8.99 (1H, *s*, H(2)), 11.92/13.69 (1H, *s*, NH); MS/EI *m*/*z* (int.rel.): 280 (57), 279 ($M^{\bullet+}$, 99), 278 (21), 250 (10), 174 (24), 173 (100), 159 (16), 158 (23), 131 (37), 130 (44), 121 (44), 92 (11), 91 (24), 77 (12), 65 (20).

2.2.6. N-(3,4-Dimethoxyphenyl)-4-oxo-4H-1-benzopyran-3-carboxamide (22)

Yield: 50%; MP: 248–254 °C; ^{1}H NMR (CDCl3): 3.77 (3H, *s*, 3′-OCH_3), 3.85 (3H, *s*, 4′-OCH_3), 7.01 (1H, *d*, *J* = 8.6, H(6′)), 7.14 (1H, *dd*, *J* = 8.6, 1.6, H(5′)), 7.37–7.30 (3H, *m*, H(6), H(8), H(2′)), 7.73–7.68 (1H, *m*, H(7)), 7.96 (1H, *d*, *J* = 7.7, H(5)), 8.86/8.83 (1H, *s*, H(2)), 11.82/13.58 (1H, *s*, NH), 13.58 (0.7 H, *s*, NH); MS/EI *m*/*z* (int.rel.): 326 (21), 325 ($M^{\bullet+}$, 100), 311 (10), 310 (63), 207 (60), 173 (62), 121 (17), 93 (20), 79 (15), 77 (15).

The structural elucidation of the other carboxamides was described elsewhere [14,15].

2.3. Radioligand binding assays

2.3.1. CHO membrane preparation

All the pharmacological methods including in membrane preparation for radioligand binding experiments followed the procedures as described earlier [16].

Membranes for radioligand binding were prepared from cells stably transfected with the human adenosine receptor subtypes (A_1, A_{2A}, and A_3 expressed on CHO cells) in a two-step procedure. In the first low-speed step (1000 × *g* for 4 min), the cell fragments and nuclei were removed. After that, the crude membrane fraction was sedimented from the supernatant at 100,000 × *g* for 30 min. The membrane pellet was then resuspended in the specific buffer used for the respective binding experiments, frozen in liquid nitrogen, and stored at −80 °C. For the measurement of the adenylyl cyclase activity in A_{2B} receptor expressed on CHO cells, only one step of centrifugation was used in which the homogenate was sedimented for 30 min at 54,000 × *g*. The resulting crude membrane pellet was resuspended in 50 mM Tris–HCl, pH 7.4 and immediately used for the adenylyl cyclase assay.

2.3.2. Human cloned A_1, A_{2A}, A_3 adenosine receptor binding assay

Binding of [^{3}H]CCPA (2-chloro-N^6-cyclopentyladenosine, GE Healthcare, Freiburg, Germany) to CHO cells transfected with the human recombinant A_1 adenosine receptor was performed as previously described [16]. Competition experiments were performed for 3 h at 25 °C in 200 μL of buffer containing 1 nM [^{3}H]CCPA, 0.2 U/mL adenosine deaminase, 20 μg of membrane protein in 50 mM Tris/HCl, pH 7.4 and tested compound in different concentrations. Nonspecific binding was determined in the presence of 1 mM theophylline and amounted to <5% of total binding [16].

Binding of [^{3}H]NECA (*N*-ethylcarboxamidoadenosine, GE Healthcare, Freiburg, Germany) to CHO cells transfected with the human recombinant A_{2A} adenosine receptors was performed following the conditions as described for the A_1 receptor binding [16]. In the competition experiments, samples containing a protein amount of 50 μg, 30 nM [^{3}H]NECA and tested compound in different concentrations were incubated for 3 h at 25 °C. Nonspecific binding was determined in the presence of 100 μM R-PIA (R-N6-phenylisopropyladenosine) and represented about 50% of total binding [16].

Binding of [^{3}H]HEMADO (2-(1-hexynyl)-*N*-methyladenosine, Tocris, Bristol, UK) to CHO cells transfected with the human recombinant A_3 adenosine receptors was carried out as previously described [16,17].

The competition experiments were performed for 3 h at 25 °C in buffer solution containing 1 nM [^{3}H]HEMADO, 20 μg membrane protein in 50 mM Tris–HCl, 1 mM EDTA (ethylenediaminotetraacetate), 10 mM $MgCl_2$, pH 8.25 and tested compound in different concentrations. Nonspecific binding was determined in the presence of 100 μM R-PIA and was below 2% of total binding [17].

All incubations were done in 96 well microplates with filter bottoms allowing for separation of bound and free ligand by filtration. Membranes with bound ligand were washed with icecold buffer to remove unbound ligand [16,17]. K_i values from competition experiments were calculated with the program SCTFIT [19] and are reported as geometric means of at least three independent experiments with 95% confidence limits [16,17].

2.3.3. Adenylyl cyclase activity

Because of the lack of a suitable radioligand for hA_{2B} receptor in binding assay, the potency of antagonists at A_{2B} receptor (expressed on CHO cells) was determined in adenylyl cyclase experiments instead. The procedure was carried out as described previously with minor modifications [16]. Membranes were incubated with about 150,000 cpm of [α-^{32}P]ATP (Hartmann-Analytic, Braunschweig, Germany) for 20 min in the incubation mixture as described [16] without EGTA and NaCl. For agonists, the EC_{50} values for the stimulation of adenylyl cyclase were calculated with the Hill equation. Hill coefficients in all experiments were near unity. IC_{50} values for concentration-dependent inhibition of NECA-stimulated adenylyl cyclase caused by antagonists were calculated accordingly. Dissociation constants (K_i) for antagonist were then calculated from the Cheng and Prusoff equation [18].

2.4. Molecular modeling

All modeling studies were carried out on a 20 CPU (Intel Core2 Quad CPU 2.40 GHz) Linux cluster. Homology modeling, energy calculation, and analyses of docking poses were performed using the Molecular Operating Environment (MOE, version 2008.10) suite [20]. The software package MOPAC (version 7) [21], implemented in MOE suite, was utilized for all quantum mechanical calculations. Docking simulation was performed using GOLD suite [21].

2.4.1. Homology models of hA_3 AR

Based on the assumption that GPCRs share similar TM boundaries and overall topology, a homology model of the hA_3 adenosine receptor was constructed, as previously reported [22,23], based on a template of the recently published crystal structure of hA_{2A} receptor (PDB code: 3EML) [24].

The numbering of the amino acids follows the arbitrary scheme by Ballesteros and Weinstein. According to this scheme, each amino acid identifier starts with the helix number, followed by the position relative to a reference residue among the most conserved amino acid in that helix. The number 50 is arbitrarily assigned to the reference residue [25].

Firstly, the amino acid sequences of TM helices of the hA_3 receptor were aligned with those of the template, guided by the highly conserved amino acid residues, including the DRY motif (Asp3.49, Arg3.50, and Tyr3.51) and three proline residues (Pro4.60, Pro6.50, and Pro7.50) in the TM segments of GPCRs. The same boundaries were applied for the TM helices of hA_3 receptor as they were identified from the 3D structure for the corresponding sequences of the template, the coordinates of which were used to construct the seven TM helices for hA_3 receptor. Then, the loop domains were constructed by the loop search method implemented in MOE on the basis of the structure of compatible fragments found in the Protein Data Bank. In particular, loops were modeled first in random order. For each loop, a contact energy function analyzed the list of candidates collected in the segment searching stage, taking into account all atoms already modeled and any atoms specified by the user as belonging to the model environment. These energies were then used to make a Boltzmann-weighted choice from the candidates, the coordinates of which were then copied to the model. Subsequently, the side chains were modeled using a library of rotamers generated by systematic clustering of the Protein Data Bank data, using the same procedure. Side chains belonging to residues whose backbone coordinates were copied from a template and were modeled first, followed by side chains of modeled loops. Outgaps and their side chains were modeled last. Special caution has to be given to EL2 because amino acids of this loop could be involved in direct interactions with the ligands. A driving force to the peculiar fold of the EL2 loop might be the presence of a disulfide bridge between cysteines in TM3 and EL2. Since this covalent link is conserved in both hA_{2A} and hA_3 receptors, the EL2 loop was modeled using a constrained geometry around the EL2-TM3 disulfide bridge. The constraints were applied before the construction of the homology model, in particular during the sequence alignment, selecting the cysteine residues involved in the disulfide bridge in hA_{2A} to be constrained with the corresponding cysteine residues in hA_3 sequence. In particular, Cys166 (EL2) and Cys77 (3.25) of the hA_{2A} receptor were constrained, respectively, with Cys166 (EL2) and Cys83 (3.25) of the hA_3 receptor. During the alignment, MOE-Align attempted to minimize the number of constraint violations. Then, after running the homology modeling, the presence of the conserved disulfide bridge in the model was manually checked. After the heavy atoms were modeled, all hydrogen atoms were added using the Protonate 3D methodology part of the MOE suite. This application assigned a protonation state for each chemical groups that minimized the total free energy of the system (taking titration into account) [26].

Protein stereochemistry evaluation was then performed by several tools (Ramachandran plot; backbone bond lengths, angles and dihedral plots; clash contacts report; rotamers strain energy report) implemented in MOE suite [20].

2.4.2. Molecular docking of adenosine receptors antagonists

Ligand structures were built using MOE-builder tool, part of the MOE suite [20], and were subjected to MMFF94x energy minimization until the rms of conjugate gradient was <0.05 kcal/mol Å^{-1}. Partial charges for the ligands were calculated using PM3/ESP methodology.

Four different programs have been used to calibrate our docking protocols: MOE-Dock [20], GOLD [27], Glide [28], and PLANTS [29]. In particular, ZM-241385 was re-docked into the crystal structure of the hA_{2A} adenosine receptor (PDB code: 3EML) with different docking algorithms and scoring functions, as already described [22]. Then, RMSD values between predicted and crystallographic positions of ZM-241385 were calculated for each of the docking algorithms. The results showed that docking simulations performed with GOLD gave the lowest RMSD value, the lowest mean RMSD value and the highest number of poses with RMSD value <2.5 Å.

On the basis of the best docking performance, all antagonist structures were docked into the hypothetical TM binding site of the hA_3 AR model and that of the hA_{2A} AR crystal structure, by using the docking tool of the GOLD suite [27]. Searching was conducted within a user-specified docking sphere, using the Genetic Algorithm protocol and the GoldScore scoring function. GOLD

performs a user-specified number of independent docking runs (25 in our specific case) and writes the resulting conformations and their energies in a molecular database file. The resulting docked complexes were subjected to MMFF94x energy minimization until the rms of conjugate gradient was <0.1 kcal/mol Å^{-1}. Charges for the ligands were imported from the MOPAC output files using PM3/ESP methodology.

Prediction of antagonist–receptor complex stability (in terms of corresponding pK_i value) and the quantitative analysis for non-bonded intermolecular interactions (H-bonds, transition metal, water bridges, hydrophobic, electrostatic) were calculated and visualized using several tools implemented in MOE suite [20].

Electrostatic and hydrophobic contributions to the binding energy of individual amino acids have been calculated as implemented in MOE suite [20]. In order to estimate the electrostatic contributions, atomic charges for the ligands were calculated using PM3/ESP methodology. Partial charges for protein amino acids were calculated on the basis of the AMBER99 force field.

3. Results and discussion

3.1. Chemistry

Two series of novel chromone carboxamides placed at positions C2 (compounds **2**–**13**) and C3 (compounds **15**–**26**) of the γ-pyrone ring were synthesized using chromone carboxylic acids (compounds **1** or **14**) as starting materials (Scheme 1).

Carboxylic acids may be converted into carboxamides by treating them with amines. However, the direct reaction does not occur spontaneously at ambient temperature, with the necessary elimination of water only taking place at high temperatures [30,31]. In order to activate carboxylic acids, one can use so-called coupling reagents that act as stand-alone reagents to generate compounds such as acid chlorides, (mixed) anhydrides, carbonic anhydrides or active esters [31].

The synthetic strategy used in this work is depicted in Scheme 1. Briefly the synthesis of the chromone carboxamide derivatives was based on a one-pot condensation with the activation *in situ* of the carboxylic acid function using a coupling reagent under mild reaction conditions. The coupling reagents selected for carboxylic acid activation were organophosphoric compounds, namely (benzotriazol-1-yloxy)tris(dimethylamino) phosphonium hexafluorophosphate (BOP) and (benzotriazol-1-yloxy) tripyrrolidinophosphonium hexafluorophosphate (PyBOP) [31]. In all the reactions, *N*,*N*-diisopropylethylamine (DIPEA) was used instead of the classic triethylamine since a significant yield increase was observed due mainly to an improvement in the purification steps [13].

The synthetic procedure has an advantage over the Schotten–Baumann reaction since it avoids the step of generation of an acyl halide with reagents such as thionyl chloride or phosphorus pentachloride, circumventing some of the drawbacks related to the use of this type of reagents, namely the ring-opening of the benzopyran nucleus [32]. Furthermore, phosphonium salts (BOP or PyBOP) were selected as coupling reagents since some of the side reactions described with the employment of carbodiimides are avoided facilitating product purification with improvement of the yield of the reaction [31].

3.2. Pharmacology

3.2.1. Binding affinity at human A_1, A_{2A}, and A_3 adenosine receptors

The affinity of the new potential antagonists for the human adenosine receptor subtypes hA$_1$, hA$_{2A}$, hA$_3$ (expressed in Chinese hamster ovary (CHO) cells) was determined in radioligand competition experiments [16–19]. In this assay, we measured the displacement of: (i) specific [^{3}H]CCPA binding at hA$_1$ receptors, (ii) specific [^{3}H]NECA binding at hA$_{2A}$ and [^{3}H]HEMADO binding hA$_3$ receptors. The data were expressed as K_i (dissociation constant), which was calculated with the program SCTFIT [19], and given as geometric means of at least three experiments, including 95% confidence intervals. The receptor binding affinities of the synthesized compounds (**2**–**13** and **15**–**26**) are reported in Tables 1 and 2, respectively.

3.2.2. Adenylyl cyclase activity

Because of the lack of a suitable radioligand for hA$_{2B}$ receptor in binding assay, the potency of antagonists at hA$_{2B}$ receptor (expressed on CHO cells) was determined in adenylyl cyclase experiments instead. The procedure was carried out as described previously in Klotz et al. with minor modifications [16]. In this

Table 1
Affinity (K_i, nM) of chromones **1**–**13** in radioligand binding assays at human A$_1$, A$_{2A}$ and A$_3$ adenosine receptors.

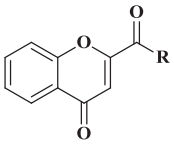

Compound	R	hA$_1$	hA$_{2A}$	hA$_3$	Selectivity	
		K_i (nM)	K_i (nM)	K_i (nM)	hA$_1$/hA$_3$	hA$_{2A}$/hA$_3$
1	OH	>100,000	>100,000	>100,000	–	–
2	NH–Ph	>100,000	>100,000	14,200 (11,800–17,100)	>7.0	>7.0
3	NH–C$_6$H$_{11}$	>100,000	>100,000	38,700 (27,400–54,700)	>2.6	>2.6
4	NH–C$_3$H$_7$	>100,000	>100,000	>100,000	–	–
5	NH–(4′–OH–Ph)	>100,000	28,300 (19,600–40,700)	46,300 (38,100–56,300)	>2.2	0.61
6	NH–(4′–OCH$_3$–Ph)	>100,000	>100,000	9580 (7600–12,100)	>10	>10
7	NH–(4′–CH$_3$–Ph)	>100,000	>100,000	15,800 (12,200–20,400)	>6.3	>6.3
8	NH–(3′–OH–4′–OCH$_3$–Ph)	>100,000	35,700 (32,700–39,100)	15,400 (10,100–23,400)	>6.5	2.3
9	NH–(3′–OCH$_3$–4′–OCH$_3$–Ph)	>100,000	>100,000	27,900 (18,300–42,700)	>3.6	>3.6
10	NH–(4′–Cl–Ph)	>100,000	>100,000	>100,000	–	–
11	NH–(4′–OCF$_3$–Ph)	>100,000	>100,000	>100,000	–	–
12	NH–(4′–CF$_3$–Ph)	>100,000	>100,000	>100,000	–	–
13	NH–(4′–NO$_2$–Ph)	>100,000	>100,000	>100,000	–	–

Table 2
Affinity (Ki, nM) of chromones **14–26** in radioligand binding assays at human A_1, A_{2A} and A_3 adenosine receptors.

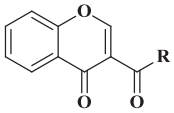

Compound	R	hA_1	hA_{2A}	hA_3	Selectivity	
		K_i (nM)	K_i (nM)	K_i (nM)	hA_1/hA_3	hA_{2A}/hA_3
14	OH	>100,000	>100,000	>100,000	–	–
15	NH–Ph	>100,000	>100,000	>100,000	–	–
16	NH–C_6H_{11}	18,400 (16,600–20,400)	26,900 (18,300–39,600)	71,300 (66,000–77,100)	0.26	0.38
17	NH–C_3H_7	19,300 (18,400–20,200)	41,600 (32,400–53,500)	40,800 (37,000–44,900)	0.47	1.0
18	NH–(4′–OH–Ph)	10,400 (8870–12,300)	22,100 (20,100–24,400)	8,860 (7460–10,500)	1.2	2.5
19	NH–(4′–OCH_3–Ph)	18,600 (14,500–23,800)	10,100 (8660–11,900)	6070 (4710–7830)	3.1	1.7
20	NH–(4′–CH_3–Ph)	>100,000	>100,000	16,600 (15,600–17,600)	>6.0	>6.0
21	NH–(3′–OH–4′–OCH_3–Ph)	8590 (7240–10,200)	6850 (6220–7550)	3680 (2770–4900)	2.3	1.9
22	NH–(3′–OCH_3–4′–OCH_3–Ph)	11,700 (10,300–13,300)	12,400 (10,200–15,000)	6690 (5610–7980)	1.8	1.9
23	NH–(4′–Cl–Ph)	25,600 (10,400–32,200)	17,400 (13,700–22,200)	16,400 (15,700–17,100)	1.6	1.1
24	NH–(4′–OCF_3–Ph)	>100,000	>100,000	>100000	–	–
25	NH–(4′–CF_3–Ph)	>100,000	>100,000	>100000	–	–
26	NH–(4′–NO_2–Ph)	>100,000	14,300 (10,500–19,500)	3750 (3530–3980)	>26	3.8

assay, the NECA-stimulated adenylyl cyclase activity was inhibited with increasing concentrations of antagonist. As a result, cAMP (cyclic adenosine monophosphate) production was inhibited in a concentration-dependent fashion, and IC_{50} and K_i values, respectively, were determined.

3.3. Molecular modeling

The recently published crystal structure of the human A_{2A} adenosine receptor, in complex with the antagonist ZM241385 (PDB code: 3EML) [24] provides a new template to perform homology modeling of other GPCRs and in particular of adenosine receptors. Therefore we built up a homology model of the hA_3 receptor based on the crystal structure of the hA_{2A} receptor (methodological details were summarized in Section 2.4.1) [22,23].

In the process of selecting a reliable docking protocol to be employed in the following docking studies of these new derivatives, we have evaluated the ability of different docking softwares in reproducing the crystallographic pose of ZM241385 inside the binding cavity of human A_{2A} receptor. As reported in Section 2.4.2, among the four different types of programs used to calibrate our docking protocol, the Gold programs was finally chosen since it showed the best performance with regard to the calculated RMSD values relative to the crystallographic pose of ZM241385 [22].

Consequently, based on the selected docking protocol, we performed docking simulations to identify the hypothetical binding mode of the newly synthesized derivatives inside the human A_{2A} and A_3 adenosine receptors.

3.4. Structure–affinity relationship studies

Chromone carboxamide derivatives (**2–13** and **15–26**) of the chromone carboxylic acids (compounds **1** and **14**) were obtained in a one pot reaction and with good yields (45–85%) (Scheme 1). Their affinity to bind to human A_1, A_{2A} and A_3 adenosine receptors (AR) expressed in CHO cells (compounds **2–13** in Table 1 and compounds **15–26** in Table 2) was determined. Due to the lack of a useful radioligand for hA_{2B} AR, the inhibition of NECA-stimulated adenylyl cyclase activity by chromone carboxylic acids and carboxamides was determined. For all the tested compounds no measurable activity (K_i > 100,000 nM) was detected.

The binding assays data clearly show that chromone carboxylic acids (compounds **1** and **14**) are devoid of activity and the corresponding carboxamides derivatives are compounds with diverse affinity and selectivity toward human A_1, A_{2A} and A_3 AR (Tables 1 and 2).

A more cautious look on the data allows to conclude that the affinity and/or selectivity of chromone carboxamides is influenced by the relative position of the carbonyl function of the carboxamide group on the benzopyran nucleus and by the type of amine (aromatic, cyclic and aliphatic) that is located in the nitrogen atom. In general, it can be also inferred that the presence of electron donators or withdrawing groups on the phenyl substituent of the carboxamide also modulate the affinity and selectivity of chromone carboxamides for the subtypes of ARs.

From the data the following specific conclusions can be drawn:

a) For carboxamides located in position 2 of the pyran nucleus (compounds **2–13**): the presence of a phenyl (compound **2**) or a cyclohexyl substituent (compound **3**) is tolerated and a fair affinity for A_3 AR is observed. However, no binding was detected with a linear alkyl substituent (compound **4**). These observations allow to infer that probably in this type of systems the spatial volume of the substituent is an important feature.The presence of electron withdrawing substituents in the phenyl ring located in the nitrogen atom, such as chlorine (compound **10**), trifluormethoxy (compound **11**), trifluormethyl (compound **12**) or nitro (compound **13**) groups in *para* position give rise to a lack of affinity for all the adenosine receptors subtypes.

   On other hand the presence of electron donators in the phenyl ring located in the nitrogen atom, in *para* position, (compounds **5–9**) result in the display of a noticeable affinity/selectivity for the A_3 AR.

b) For carboxamides located in position 3 of the pyran nucleus (compounds **15–26**): in this chromone carboxamide isomeric series the conclusions were not as straightforward as in the series with a 2-substituted pyran. However, for this type of benzopyran derivatives the results show that similar to the 2-substituted isomers the presence of electron donating groups in the phenyl substituent increase the affinity and selectivity for the human A_3 AR (compounds **18–22**). It is to note that compounds **18** and **19** exhibit micromolar affinity for all the studied receptors but without a significant selectivity. With

exception of compound **26** with a nitro function in *para* position, that have high A_3 AR affinity, the chromone derivatives with electron withdrawing groups have no measurable affinity for adenosine receptors (compound **24** and **25**). Moreover, it is important to highlight that compounds **21** and **26** present the best affinity for A_3 receptor with a K_i = 3684 nM and K_i = 3750 nM, respectively.

A molecular modeling investigation was performed for all the newly synthesized analogues, in order to identify their hypothetical binding modes at both the crystallographic structure of hA_{2A} AR and the hA_3 AR model. The analysis was extended to docking simulations and *per residue* electrostatic and hydrophobic contributions.

The first important consideration is that almost all the new analogues showed different possible binding poses at both the hA_{2A} AR and the hA_3 AR. In fact, even if all ligands made contacts mainly with residues belonging toTM2, TM3, TM6, TM7, and EL2, they can accommodate different orientations inside the binding pockets.

Fig. 1 shows the selected binding modes of compound **21**, a chromone with the carboxamide located in position 3 of the pyran nucleus, obtained after docking simulations at the hA_{2A} AR and the hA_3 AR. Among all the herein reported derivatives, compound **21** possesses the highest affinity at both receptors (K_i hA_{2A} = 6850 nM, K_i hA_3 = 3684 nM). At both receptor subtypes ligand-recognition occurred in the upper region of the TM bundle, and the chromone nucleus was surrounded by TMs 3, 5, 6, 7.

The hypothetical binding pose of compound **21** at the hA_{2A} AR (Fig. 1, panel A) showed an H-bonding interaction with Asn253 (6.55) and a stabilizing interaction with Phe168 (EL2). Interestingly, the important role in ligand binding of these two residues was previously revealed by site-directed mutagenesis studies [33,34] and by the crystallographic binding pose of ZM241385 inside the hA_{2A} AR binding pocket [24].

Moreover, the hydroxyl group on the phenyl ring of compound **21** interacted with Tyr271 (7.36), forming a weak H-bond. Finally, the ligand also formed hydrophobic interactions with some residues of the binding site, including Leu85 (3.33), Trp246 (6.48), Leu249 (6.51), Tyr271 (7.36) and Ile274 (7.39).

On the other hand, the docking pose of compound **21** at the hA_3 AR was located in the same region of the TM bundle as at the hA_{2A} AR, but the orientation of the ligand was different (Fig. 1, Panel B). In this case, the ligand formed two H-bonds with Asn250 (6.55) and a stabilizing interaction with Phe168 (EL2). Moreover, the complex is stabilized by hydrophobic interactions occurring between the ligand and some residues of the binding site, such as Leu91 (3.33), Trp243 (6.48), Leu246 (6.51) and Leu264 (7.35).

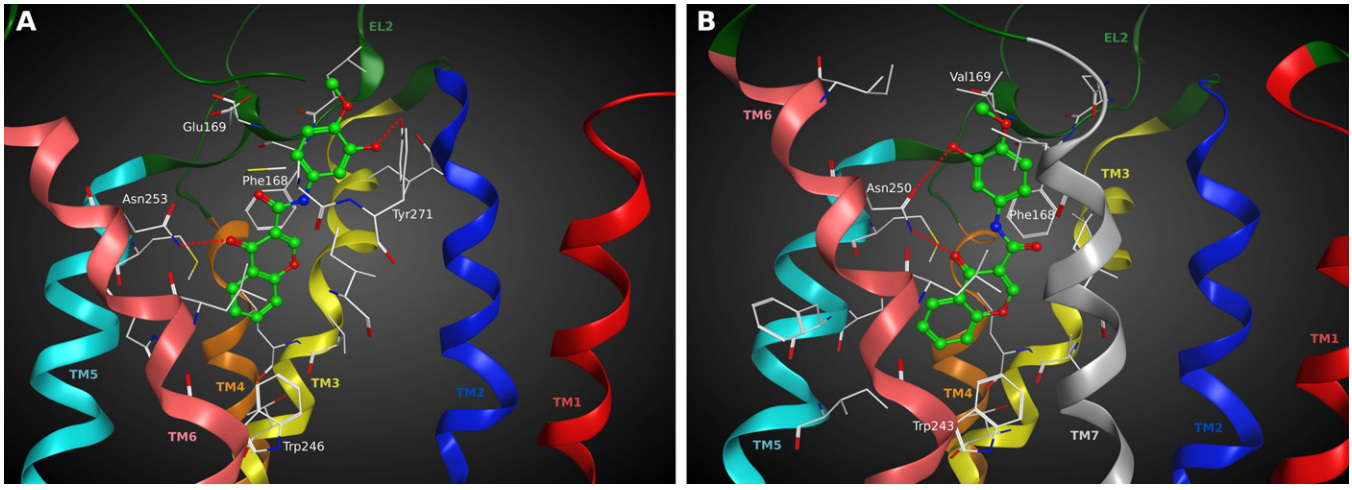

Fig. 1. Hypothetical binding modes of compound **21** obtained after docking simulations: (A) inside the hA_{2A} AR binding site; (B) inside the hA_3 AR binding site. Poses are viewed from the membrane side facing TM6, TM7, and TM1. In panel A, the view of TM7 is omitted. Side chains of some amino acids important for ligand recognition and H-bonding interactions are highlighted. Hydrogen atoms are not displayed.

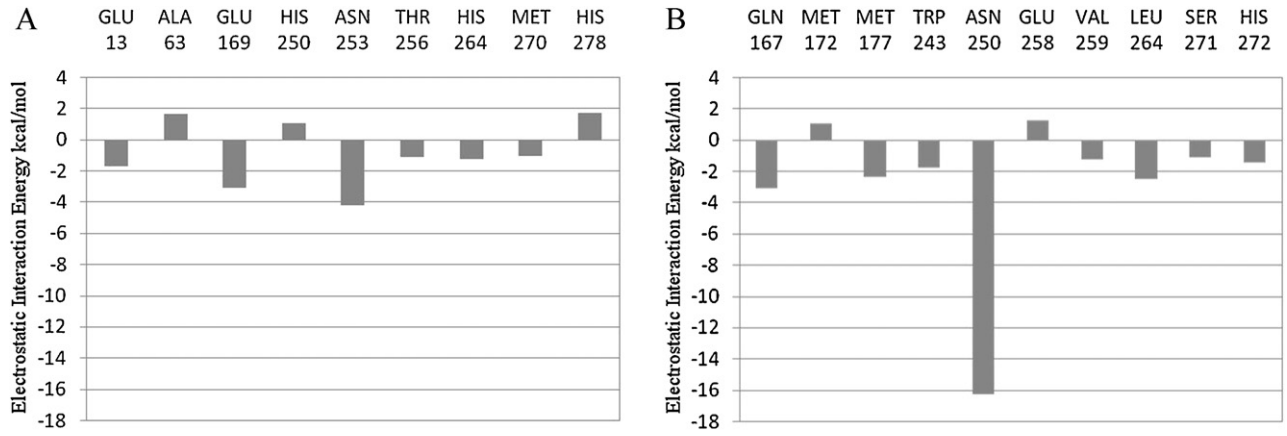

Fig. 2. Calculated electrostatic interaction energy (in kcal/mol) between the ligand and each single amino acid involved in ligand recognition observed from the hypothetical binding modes of compound **21** inside (A) hA_{2A} AR and (B) hA_3 AR binding sites.

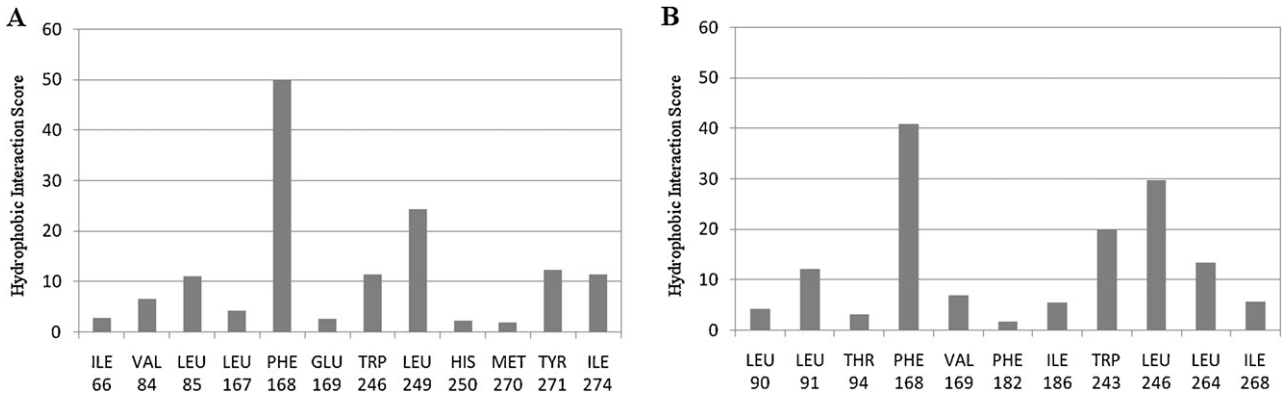

Fig. 3. Calculated hydrophobic interaction scores (in arbitrary hydrophobic units) between the ligand and each single amino acid involved in ligand recognition observed from the hypothetical binding modes of compound **21** inside (A) hA_{2A} AR and (B) hA_3 AR binding sites.

Another antagonist of this series with affinity at the hA_3 AR comparable to compound **21** is compound **26** (K_i hA_3 = 3750 nM). The binding orientation, obtained after docking simulation, of this ligand at this receptor is very similar to the one observed for compound **21** (data not shown). In this case, compound **26** formed one H-bonding interaction with Asn250 (6.55) and a stabilizing interaction with Phe168 (EL2).

Analyzing the calculated electrostatic contribution *per residue* to the whole interaction energy for both the complexes between compound **21** and these two adenosine receptor subtypes (Fig. 2), the main stabilizing factor was found to be related to Asn 6.55 (Asn253 in hA_{2A} AR and Asn250 in hA_3 AR), due to the H-bonding interactions with the ligand above described. However, the calculated electrostatic contribution of this Asn residue is much more stabilizing for the hA_3 AR complex (−16 kcal/mol for hA_3 AR complex compared to −4 kcal/mol for hA_{2A} AR complex).

As shown in Fig. 3, the hydrophobic interaction scores patterns showed the strongest stabilizing contribution corresponding to the interactions of the ligand with Phe168 (EL2) at both receptors.

In conclusion, at the hA_{2A} AR compound **21** was able to interact with Asn253 (6.55) and Phe168 (EL2), important residues in ligand recognition, but it did not form strong interaction with Glu169 (EL2), another residue with an important role in ligand binding as revealed by the crystallographic binding pose of ZM241385 inside the hA_{2A} AR binding pocket [24]. At the hA_3 AR compound **21** formed stronger, but still not optimal, interactions with the residues of the binging site, and in particular with Asn250 (6.55). This difference could be the reason for the higher affinity of this compound for this adenosine receptor subtype compared to the hA_{2A} subtype.

On the whole, the proposed binding modes reflect the ability of compound **21** to bind both hA_{2A} and hA_3 adenosine receptor subtypes with K_i in the low micromolar range and without a very good selectivity profile.

4. Conclusions

Evidence was acquired to demonstrate that chromone is a valid scaffold for the design of novel adenosine receptor ligands. The easy synthetic accessibility and the decoration capability of chromones make them "privileged" scaffolds.

From this study and on the basis of the obtained structure–activity relationships it was concluded that chromone carboxamides represent a novel class of AR ligands. The most remarkable chromones were compounds **21** and **26** that present a better affinity for A_3 AR (K_i = 3680 nM and K_i = 3750 nM, respectively). The results obtained so far pointed out a crucial and undisclosed role of the presence of an amide substituent of the pyrone ring and that the type of substituent on the aromatic ring of the chromone amide side chain is crucial for the optimization of affinity and selectivity. Receptor-driven molecular modeling studies provide information on the binding/selectivity data of the chromone. The data so far acquired are instrumental for future optimization of chromone carboxamide lead as a selective A_3AR antagonist.

Acknowledgments

This work was supported by the Foundation for Science and Technology (FCT), Portugal (project PTDC/QUI/70359/2006 and PTDC/QUI-QUI/113687/2009).

A. Gaspar (SFRH/BD/43531/2008) and FB (SFRH/BSAB/1090/2010) thanks FCT grants. The work coordinated by S.M. was carried out with financial support from the University of Padova, Italy, and the Italian Ministry for University and Research (MIUR), Rome, Italy. S.M. is very grateful to Chemical Computing Group Inc. (Montreal, Quebec, Canada) for the scientific and technical partnership.

References

[1] Erik S. Mechanisms of cancer cell invasion. Curr Opin Genetics Dev 2005;15:87–96.
[2] Aggarwal BB, Sethi G, Baladandayuthapani V, Krishnan S, Shishodia S. Targeting cell signaling pathways for drug discovery: an old lock needs a new key. J Cell Biochem 2007;102:580–92.
[3] Gessi S, Merighi S, Sacchetto V, Simioni C, Borea PA. Adenosine receptors and cancer. BBA – Biomembr 2011;1808:1400–12.
[4] Fishman P, Bar-Yehuda S, Varani K, Gessi S, Merighi S, Borea PA. Agonists and antagonists: molecular mechanisms and therapeutic applications. In: Borea PE, editor. A3 adenosine receptors from cell biology to pharmacology and therapeutics. Dordrecht Heidelberg London New York: Springer; 2010.
[5] Gessi S, Merighi S, Varani K, Leung E, Mac Lennan S, Borea PA. The A_3 adenosine receptor: an enigmatic player in cell biology. Pharmacol Ther 2008;117:123–40.
[6] Fishman P, Jacobson KA, Ochaion A, Cohen S, Bar-Yehuda S. The anti-cancer effect of A_3 adenosine receptor agonists: a novel, targeted therapy. Immunol Endocr Metabol Agents Med Chem 2007;7:298–303.
[7] Hasko G, Linden J, Cronstein B, Pacher P. Adenosine receptors: therapeutic aspects for inflammatory and immune diseases. Nat Rev Drug Discov 2008;7:759–70.
[8] Baraldi PG, Romagnoli R, Saponaro G, Baraldi S, Tabrizi MADP. A3 adenosine receptor antagonists: history and future perspectives. In: Borea PA, editor. A3 adenosine receptors from cell biology to pharmacology and therapeutics. Dordrecht Heidelberg London New York: Springer; 2010.
[9] DeNinno MP, Masamune H, Chenard LK, DiRico KJ, Eller C, Etienne JB, et al. The synthesis of highly potent, selective, and water-soluble agonists at the human adenosine A_3 receptor. Bioorg Med Chem Lett 2006;16:2525–7.
[10] Baraldi PG, Tabrizi MA, Gessi S, Borea PA. Adenosine receptor antagonists: translating medicinal chemistry and pharmacology into clinical utility. Chem Rev 2008;108:238–63.
[11] Jacobson KA. Introduction to adenosine receptors as therapeutic targets. In: Wilson CN, Mustafa SJ, editors. Adenosine receptors in health and disease:. Berlin Heidelberg: Springer-Verlag; 2009.

[12] Lars JSK. Drug discovery management, small is still beautiful: why a number of companies get it wrong. Drug Discov Today 2011;16:476–84.
[13] Borges F, Gaspar A, Garrido J, Milhazes N, Batoreu MC. Chromone derivatives for use as antioxidants/preservatives. PT 103665, WO 2008/104925.
[14] Gaspar A, Silva T, Yáñez M, Vina D, Orallo F, Ortuso F, et al. Chromone, a privileged scaffold for the development of monoamine oxidase inhibitors. J Med Chem 2011;54:5165–73.
[15] Gaspar A, Teixeira F, Uriarte E, Milhazes N, Melo A, Cordeiro MNDS, et al. Towards the discovery of a novel class of monoamine oxidase inhibitors: structure–property–activity and docking studies on chromone amides. ChemMedChem 2011;6:628–32.
[16] Klotz KN, Hessling J, Hegler J, Owman C, Kull B, Fredholm BB, et al. Comparative pharmacology of human adenosine receptor subtypes–characterization of stably transfected receptors in CHO cells. N-S Arch Pharmacol 1997;357: 1–9.
[17] Klotz KN, Falgner N, Kachler S, Lambertucci C, Vittori S, Volpini R, et al. [^{3}H]HEMADO–a novel tritiated agonist selective for the human adenosine A_3 receptor. Eur J Pharmacol 2007;556(1–3):14–8.
[18] Cheng Y-C, Prusoff WH. Relationship between the inhibition constant (K_I) and the concentration of inhibitor which causes 50 per cent inhibition (IC_{50}) of an enzymatic reaction. Biochem Pharmacol 1973;22:3099–108.
[19] De Lean A, Hancock AA, Lefkowitz RJ. Validation, statistical analysis of a computer modeling method for quantitative analysis of radioligand binding data for mixtures of pharmacological receptor subtypes. J Mol Pharmacol 1982;21:5–16.
[20] MOE. (Molecular Operating Environment), version 2008.10; software available from Chemical Computing Group Inc. (1010 Sherbrooke Street West, Suite 910, Montreal, Quebec, Canada H3A 2R7); http://www.chemcomp.com.
[21] Stewart JJP. MOPAC Version 7. Tokyo, Japan: Fujitsu Limited; 1993.
[22] Lenzi O, Colotta V, Catarzi D, Varano F, Poli D, Filacchioni G, et al. 2-Phenylpyrazolo[4,3-d]pyrimidin-7-one as a new scaffold to obtain potent and selective human A_3 adenosine receptor antagonists: new insights into the receptor-antagonist recognition. J Med Chem 2009;52:7640–52.
[23] Morizzo E, Federico S, Spalluto G, Human Moro S. A_3 adenosine receptor as versatile G protein-coupled receptor example to validate the receptor homology modeling technology. Curr Pharm Des 2009;15:4069–84.
[24] Jaakola V-P, Griffith MT, Hanson MA, Cherezov V, Chien EYT, Lane JR, et al. The 2.6 Angstrom crystal structure of a human A_{2A} adenosine receptor bound to an antagonist. Science 2008;322:1211–7.
[25] Ballesteros JA, Weinstein H. Integrated methods for the construction of three-dimensional models and computational probing of structure-function relations in G protein-coupled receptors. In: Stuart CS, editor. Methods in neurosciences. Academic Press; 1995. p. 366–428.
[26] Labute P. Protonate 3D: assignment of ionization states and hydrogen coordinates to macromolecular structures. Proteins Struct Funct Bioinf 2009;75:187–205.
[27] GOLD suite, version 4.0.1; software available from Cambridge Crystallographic Data Centre Cambridge Crystallographic Data Centre (12 Union Road Cambridge CB2 1EZ UK); http://www.ccdc.cam.ac.uk.
[28] Friesner RA, Banks JL, Murphy RB, Halgren TA, Klicic JJ, Mainz DT, et al. Glide: A new approach for rapid, accurate docking and scoring. 1. Method and assessment of docking accuracy. J Med Chem 2004;47:1739–49.
[29] Korb O, Stutzle T, Exner TE. Empirical scoring functions for advanced protein-ligand docking with PLANTS. J Chem Inf Model 2009;49:84–96.
[30] Allen CL, Williams JMJ. Metal-catalysed approaches to amide bond formation. Chem Soc Rev 2011;40:3405–15.
[31] Han S-Y, Kim Y-A. Recent development of peptide coupling reagents in organic synthesis. Tetrahedron 2004;60:2447–67.
[32] Ellis GP. General methods of preparing chromones. In: Chemistry of heterocyclic compounds. John Wiley & Sons, Inc.; 2008. pp. 495–555.
[33] Kim J, Wess J, van Rhee AM, Schöneberg T, Jacobson KA. Site-directed mutagenesis identifies residues involved in ligand recognition in the human A adenosine receptor. J Biol Chem 1995;270:13987–97.
[34] Jaakola V-P, Lane JR, Lin JY, Katritch V, Ijzerman AP, Stevens RC. Ligand binding and subtype selectivity of the human A_{2A} adenosine receptor. J Biol Chem 2010;285:13032–44.